New Methods for Improved Accuracy of Broad Band Free Space Dielectric Measurements

J.W. Schultz[#1], R. Geryak[#2], J.G. Maloney[*3]

[#]Compass Technology Group, USA

[*]Maloney-Solutions, USA

{[1]john.schultz, [2]ren.geryak}@compasstech.com, [3]jim@maloney-solutions.com

***Abstract* — Recent interest in communication and sensing at millimetre wave frequencies has led to a need for accurate characterization of dielectric materials for antennas and components. Historically, broad-band free space methods have suffered from poor accuracy when determining the loss tangent of very low-loss materials. This paper provides several new corrections that improve the loss tangent accuracy of these methods by over an order of magnitude. Specifically, corrections that account for beam shift and focusing effects are described and demonstrated on several dielectric materials known for their low loss. These corrections are demonstrated on both focused beam and non-focused, free-space probe measurements.**

***Keywords* — low loss dielectrics, loss tangent, free space focused beam, spot probe measurements**

I. INTRODUCTION

With the rapid growth of wireless communication and sensing, there has been increased development of technologies with ever higher frequencies. For example, high bandwidth communication has driven the opening of spectrum within the 20 to 40 GHz band, and component or antenna design requires accurate materials properties in these frequencies. The communication and sensing required for autonomous vehicles have also added new emphasis to E-band (60 to 90 GHz). Therefore, component design requires accurate dielectric properties of materials at these frequencies as well.

For millimetre wave dielectric measurements, free space quasi-optical methods are often employed because precise machining or sample preparation are not needed. Among the free-space methods, there are two approaches typically used: resonant or broad-band. The resonant approach uses a Fabry-Perot interferometer as a resonant cavity in which a specimen is placed and measured. A Gaussian tapered beam excites the cavity and the change in the resonances with and without the sample determine the real and imaginary permittivity [1].

While the Fabry-Perot method has good sensitivity for very low loss materials, it is limited to electrically thin specimens. An alternative considered in this paper is the broad-band free space method. In this case the non-resonant fixture illuminates a planer specimen on one side and receives either the reflected energy with the same feed antenna or the transmitted energy with a second antenna placed on the other side of the specimen. The antennas may be spot probes, designed to be within a few wavelengths or so of either side of the specimen [2].

While spot probes are compact, better accuracy is obtained when larger focusing elements are used with a specimen placed at the illumination focus. This provides both a confined spot illumination as well as an approximately flat phase front at the sample, approximating a far-field plane wave. Unlike the Fabry-Perot resonator, broadband methods are not restricted to thin specimens. However, broadband techniques are known for significantly less sensitivity then the Fabry-Perot for low loss tangents. Specifically, loss tangents of 0.01 or 0.02 have typically been the lower bound of broadband methods [3].

The work in this paper significantly improves the previous low-loss limitations of broad band measurements. New corrections are presented for removing measurement bias contributing to these lower bounds. The corrections can be applied to either spot probe or focused beam methods providing an order of magnitude improvement to the low-loss measurement accuracy. Furthermore, careful design and alignment of focused beam hardware provides further accuracy improvements that when combined with the analytical corrections enables loss tangents below 0.001 to be measured.

II. DIELECTRIC MEASUREMENT METHOD

A. Spot Probes

Spot probes are specialized antennas designed to illuminate a nearby area on a surface rather than the far-field gain criteria usually used to optimize antenna performance. The idea of a compact probe for free space microwave measurements goes back at least several decades. In the mid 1970s, Musil et al. used dielectric rod antennas to measure transmission through a material [4]. While this early work inserted dielectric rods in the end of horn antennas, the spot probes described here are more advanced. They consist of metallic elements and shaped dielectric material optimized together with a computational electromagnetic code. They operate over a wide band, 20 to 40 GHz, with excellent VSWR (voltage standing wave ratio), and are designed to illuminate a material specimen or surface that is 3 to 7 cm in front of the probe. The model SP2040 probes used in this work are commercially available from Compass Technology Group and pictured in Figure 1.

Measurements were done with a pair of these probes, one as transmitter and the other as receiver. They were mounted facing each other with an approximately 14 cm space between them. Planar specimens were inserted between the probes to measure phase and amplitude of the transmission coefficient. The half-power full width spot size on the specimen varies from 5 cm at 20 GHz to 2.5 cm at 40 GHz. A vector network analyser was used as the microwave source and receiver.

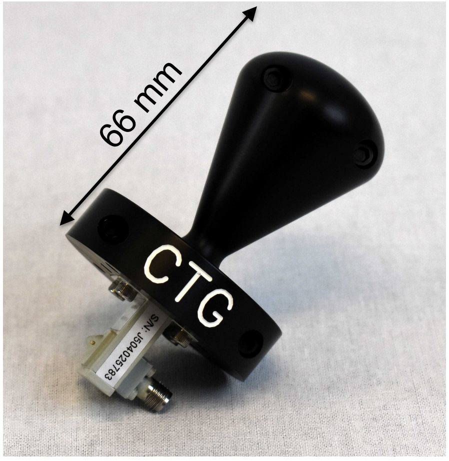

Figure 1. 20-40 GHz spot probe used for dielectric measurements

B. Focused Beam

The free space focused beam is a method that uses horn antennas with dielectric lenses or metal parabolic reflectors to focus the energy onto a specimen. These focusing elements control beam width and phase taper of the incident energy. A focus is formed in front of the lens or reflector, and a specimen is placed at the focus where the phase taper is minimized, and the fields can be approximated as plane-wave like.

For the measurements conducted in this work, lens-based focused beam fixtures were used. The focused beam system used for 60-90 GHz characterization is shown in Figure 2. It includes E-band frequency extender modules exciting waveguide horns and 150 mm diameter Rexolite lenses to create a focused beam for illuminating the material specimens. For 10 to 40 GHz measurements, a larger lens system was also used. This larger system combined open boundary quad-ridged horns (MVG QH4000) with 600 mm diameter lenses to illuminate the material specimens.

Focused beam systems such as these are quasi-optical and can be modelled with Gaussian beam optics approximations [3]. Gaussian optics accounts for the diffraction-limited spot size and models the amplitude taper of this focused spot as a Gaussian function. For a focused beam parallel to the *z*-axis, the amplitude taper, *u*, can be described at the focal point by

$$u(z = 0) = e^{\left(\frac{-r^2}{w_0^2}\right)}, \quad (1)$$

where *r* is the distance from the centre of the beam, and w_0 is the beam waist. Thus, the beam waist corresponds to the 1/e field point of the beam, which is where the power is reduced to -8.7 dB relative to the centre.

Typically, beam waist is inversely proportional to frequency or wave number. So, a general parameter to characterize a focused beam is $k_0 w_0$ where k_0 is the free-space wave number. To put this parameter in perspective, a single plane wave is infinite in extent with $k_0 w_0 = \infty$. On the other hand, a finite spot can be decomposed into a distribution of plane waves. As the spot size decreases, $k_0 w_0$ becomes smaller, and the width of the plane wave distribution increases [5]. As discussed later in this paper, a small but non-negligible source of measurement bias is "focusing error", which is related to the $k_0 w_0$ of a measurement system. In relation to the ideal plane wave assumption, the larger the $k_0 w_0$ is, the less the focusing error. The larger focused beam system (10 to 40 GHz) has a $k_0 w_0$ of approximately 12 to 16, while the smaller, 60-90 GHz focused beam system in Figure 2 has a $k_0 w_0$ of approximately 20.

Figure 2. Photograph of lens-based focused beam system for measuring materials at 60-90 GHz.

C. Data Processing and Dielectric Inversion

In free space systems, the spatially varying beam prevents conventional calibrations (e.g. Thru/Reflect/Line, etc.) from being accurate. Instead, the calibration method used here was a response measurement combined with time domain gating. The reference measurement was of the empty system, while the time domain gating minimizes multipath effects. Specifically, the frequency data are converted to time domain via an inverse Fourier transform, and a finite window is placed around the desired signal (to gate out the other noise signals). The proximity of the spot probes requires a 0.5 ns gate width to minimize the effects of probe ringing. For the longer focused beam fixtures, wider gates were employed since the multipath reflections were further away in time from the specimen.

Dielectric permittivity and loss were calculated by inverting the amplitude and phase of the transmission coefficients with an iterative routine. The theory is based on an ideal plane wave interacting with a finite thickness infinite dielectric slab at normal incidence. The usual frequency-by-frequency method based on network scattering parameters of a two-port microwave network was used, as described in [3].

III. Analytical Corrections

A. Beam Shift Correction

One potential source of bias in low loss measurements is a 'beam shift' from refraction through the sample. This effect is shown notionally in Figure 3 for the case of a diverging beam, such as the spot probes. Refraction by the specimen causes the beam to shift forward towards the receive probe.

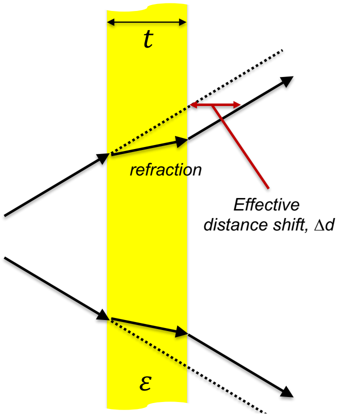

Figure 3. Sketch showing the beam shift effect from a specimen with permittivity ε and thickness *t*.

The amount of shift, Δd can be quantified by applying Snell's law to rays passing through a slab of thickness *t*, and permittivity, ε. For a directive beam, we assume small angle and the resulting beam shift is,

$$\Delta d = \mathrm{t}\left(1 - \frac{1}{\sqrt{\varepsilon}}\right). \quad (2)$$

The only other information needed to implement this correction is the dependence of transmission amplitude on distance between the transmit and receive antennas. For the spot probes, finite difference time domain simulations were done to calculate the transmission coefficient (S_{21}) versus transmit and receive separation. With these results, an interpolated table of S_{21} amplitude versus beam shift was used along with Eq. (2) to correct the measured S_{21} amplitude. An example of this correction is in Figure 4, which shows measurements of a low-loss high density polyethylene (HDPE) specimen, 6.3 mm thick. The oscillation of the amplitude versus frequency is from constructive and destructive interference between the front and back surfaces. Without correction, the peak transmission goes above 0 dB, which is non-physical. After beam shift correction, the measured amplitude is no greater than 0 dB, as expected.

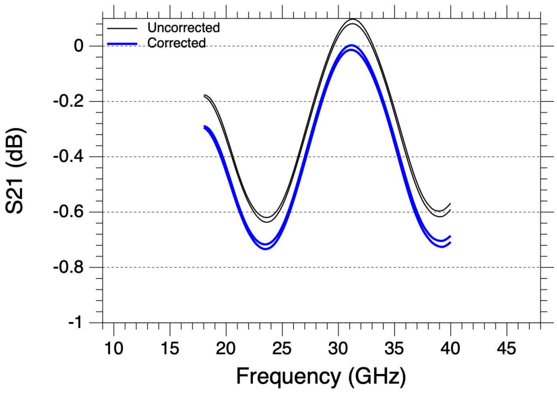

Figure 4. Measured S_{21} amplitude of 6.3 mm thick HDPE

While the illustration above shows the beam shift correction applied to spot probes, it can also be applied to a focused beam. The larger size of the focused beam systems makes computational electromagnetic simulations less practical for calculating transmission dependence on transmitter and receiver separation. For the results shown later in this paper, the S_{21} variation versus Δd was instead determined experimentally for each of the lens systems.

B. Focusing Correction

The second potential source of measurement bias investigated is from the finite spot size of a focused beam. A typical assumption is that the incident energy may be approximated as a plane wave where $k_0 w_0 \sim \infty$. In most cases the error associated with this approximation is sufficiently low in magnitude to be ignored. However, in pursuit of increased accuracy for low loss-tangent levels this bias was also evaluated, and a correction derived. As discussed above, the beam produced by a focused beam system can be described as a collection of plane waves with different wavevectors. This has the effect of tilting a small portion of the electric/magnetic field components away from the assumed transverse fields in normal incidence plane waves.

A previous analysis had considered the changes in sample interaction associated with this focusing effect [6]. This approach derived integral solutions describing the interaction of a Gaussian beam with a known slab of material. The transmitted power, P^t, is described as a function of the focused beam system parameters k_0 and w_0 as

$$P^t = k_0^2 w_0^4 \int f(k_\rho, \varepsilon) e^{-k_\rho^2 (k_0 w_0)^2/2} dk_\rho \quad (3)$$

where k_ρ is the radial wavenumber, and $f(k_\rho,\varepsilon)$ is a function containing the material-dependent transmission coefficients for TM/TE polarization, as well as the strength of the electric field.

The solutions to this integral can be approximated numerically given the focused beam parameters (i.e. $k_0 w_0$) and the material (i.e. thickness, permittivity). Most of these parameters are directly determined through external measurements, but the permittivity of the material is the unknown parameter that needs to be determined.

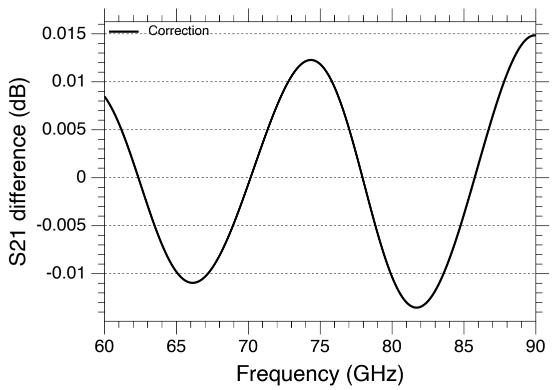

Figure 5. S_{21} amplitude focusing correction for 6.3 mm thick HDPE in E-band focused beam system

In the current algorithm, the measured S_{21} amplitude is adjusted with the beam shift and focusing corrections, and then combined with the measured phase to generate complex S_{21}

data for final inversion with the standard iterative method. Figure 5 shows an example of the focusing correction for an HDPE specimen in the E-band focused beam system.

IV. Measurement Examples

A number of low-loss materials were measured to see the accuracy limits with both spot probes and with focused beam systems using these corrections. Figure 6 shows the real part of the dielectric permittivity of a 6.3 mm thick HDPE specimen measured with the spot probes and both focused beam systems. The corresponding loss tangent is shown in Figure 7. HDPE, which is known to be very low loss, shows the lower limit of loss tangent sensitivity achieved in this work. The results show significantly more accuracy for the E-band focused beam than the below-40 GHz free space methods. Work is ongoing to identify the remaining errors in the lower frequency methods.

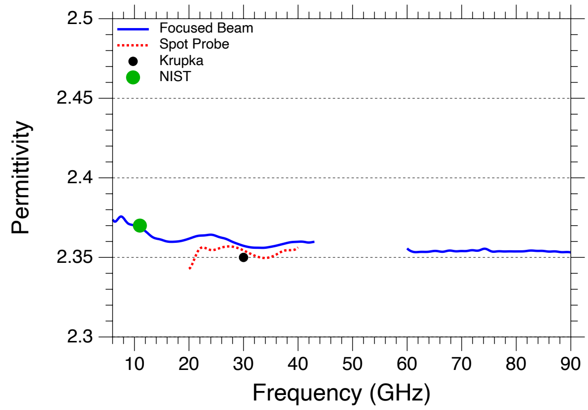

Figure 6. Real part of dielectric permittivity extracted for a 6.3 mm thick HDPE specimen. The spot probe data included a beam shift correction while the focused beam data had both beam shift and focusing corrections applied. [7-8]

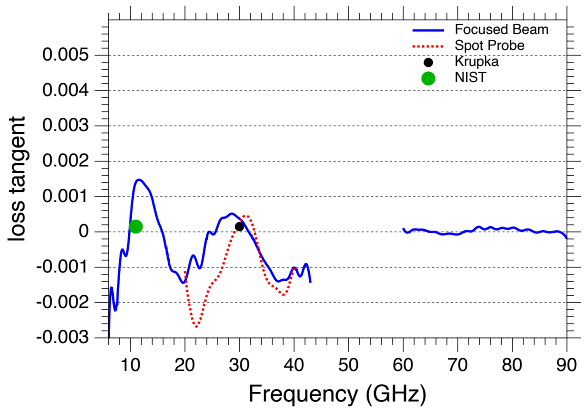

Figure 7. Dielectric loss tangent extracted for a 6.3 mm thick HDPE specimen. The spot probe data included a beam shift correction while the focused beam data had both beam shift and focusing corrections applied. [7-8]

Another example of a low, but measurable loss tangent is shown for acrylic, also known as polymethyl methacrylate (PMMA) in Figure 8. The loss tangent measured with the spot probes and focused beam systems are in good agreement with Fabry-Perot measurements described in the literature [8-10].

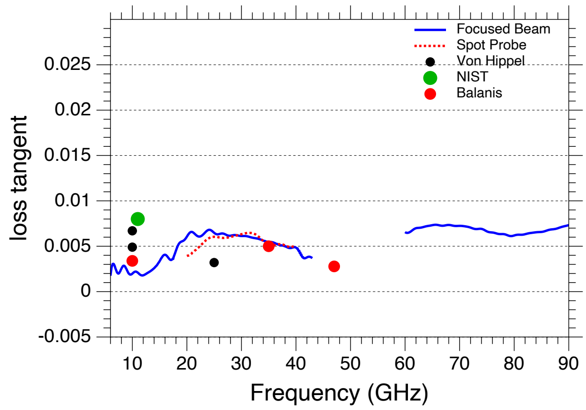

Figure 8. Dielectric loss tangent extracted for a 3.1 mm thick Acrylic specimen. The spot probe data included a beam shift correction while the focused beam data had both beam shift and focusing corrections applied. [8-10]

V. Conclusion

New corrections that account for measurement bias in broadband free space measurements were derived. These corrections were applied to improve the accuracy of spot probe and focused beam measurements. Low-loss materials were characterized with these techniques and demonstrated broad band loss tangent measurement sensitivity of less than +/- 0.002 up to 40 GHz and sensitivity of approximately +/- 0.0002 at E-band frequencies.

Acknowledgment

The authors acknowledge Zander Borders for his expert alignment of and measurements with the focused beam systems.

References

[1] C.A. Balanis, "Measurements of Dielectric Constants and Loss Tangents at E-Band Using a Fabry-Perot Interferometer," NASA Technical Note D-5583, 1969

[2] J.W. Schultz, J.G. Maloney, K.C. Maloney, R.M. Schultz, "A Comparison of Material Measurement Accuracy of RF Spot Probes to a Lens-Based Focused Beam System," Proc. 2014 AMTA Symposium, 2014

[3] J.W. Schultz, *Focused Beam Methods, Measuring Microwave Materials in Free Space*, Create-Space Publishing, 2012

[4] J. Musil, F. Zacek, A. Burger, J. Karlovsky, "New Microwave System to Determine the Complex Permittivity of Small Dielectric and Semiconducting Samples," 4th European Microwave Conference, 66-70, 1974

[5] L.E.R. Petersson, G.S. Smith, "An Estimate of the Error Caused by the Plane-Wave Approximation in Free-Space Dielectric Measurement Systems," IEEE Trans. AP, 50(6), 878-887, (2002)

[6] L.E.R. Petersson, "Analysis of Two Problems Related to a Focused Beam Measurement System," Ph.D Thesis, School of Elec. and Comp. Eng. Georgia Inst. of Tech., 2002

[7] J. Krupka, "Measurements of the Complex Permittivity of Low Loss Polymers at Frequency Range From 5 GHz to 50 GHz," IEEE Microwave and Wireless Components Lett., vol, 26(6), 464 – 466, June 2016

[8] B. Riddle, J. Baker-Jarvis, J. Krupka, "Complex Permittivity Measurements of Common Plastics over Variable Temperatures," IEEE Trans. MTT, vol 51(3), 727-733, 2003

[9] A. R. Von Hipple: Dielectric Materials and Applications, New York: Wiley, 1954

[10] C.A. Balanis, "Measurements of Dielectric Constants and Loss Tangents at E-Band Using a Fabry-Perot Interferometer," NASA Technical Note D-5583, 1969